Supplementary material for

Carbon vacancies regulation strategy for boosting the high-temperature microwave absorption performance of $(Co_{0.2}Mo_{0.2}V_{0.2}Nb_{0.2}Ta_{0.2})C_x$ high-entropy carbides

Yuping Duan*[1], Likun Niu[1], Zerui Li[1], Xiaoji Liu[1], Huifang Pang[1], Jiabin Ma[1], Jian Gong[2], Jiangang Wang[2]

1. Key Laboratory of Solidification Control and Digital Preparation Technology (Liaoning Province), School of Materials Science and Engineering, Dalian University of Technology, Dalian 116085, P.R. China

2. China-Blarus Belt and Road Joint Laboratory on Electromagnetic Environment Effect, Taiyuan 030032, P. R. China.

*Corresponding authors. E-mail address: duanyp@dlut.edu.cn (Y. Duan).

ORCID iD: 0000-0001-5599-7168

1.Supplementary Figures

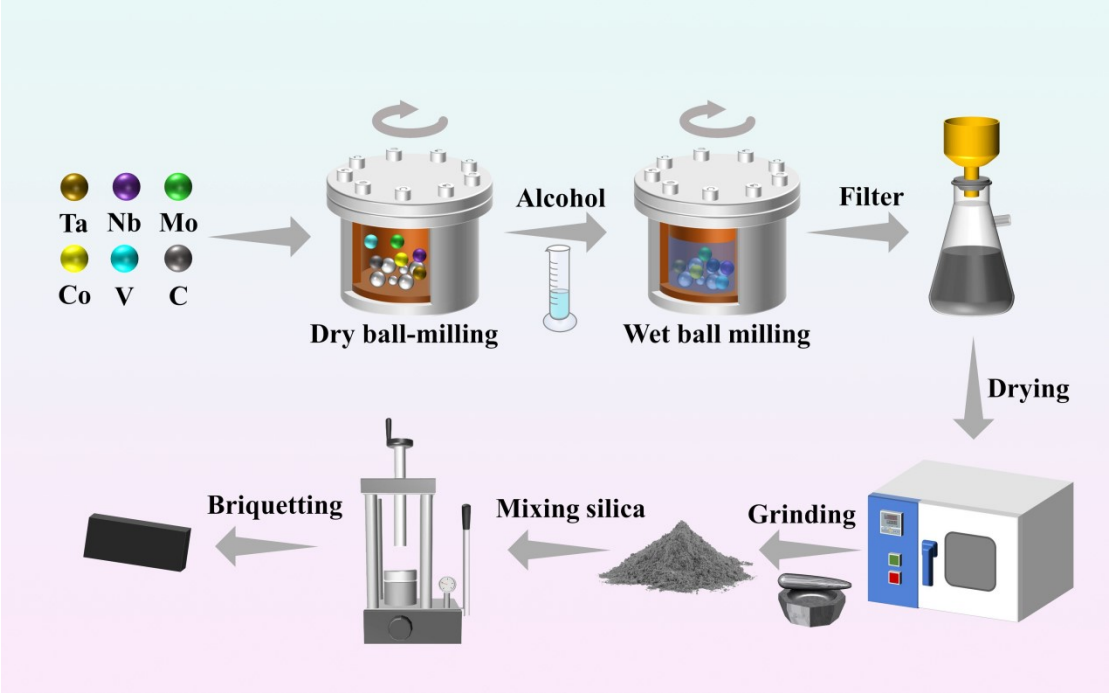

Fig. S1. Synthesis of $(Co_{0.2}Mo_{0.2}V_{0.2}Nb_{0.2}Ta_{0.2})C_x$ and test sample preparation process.

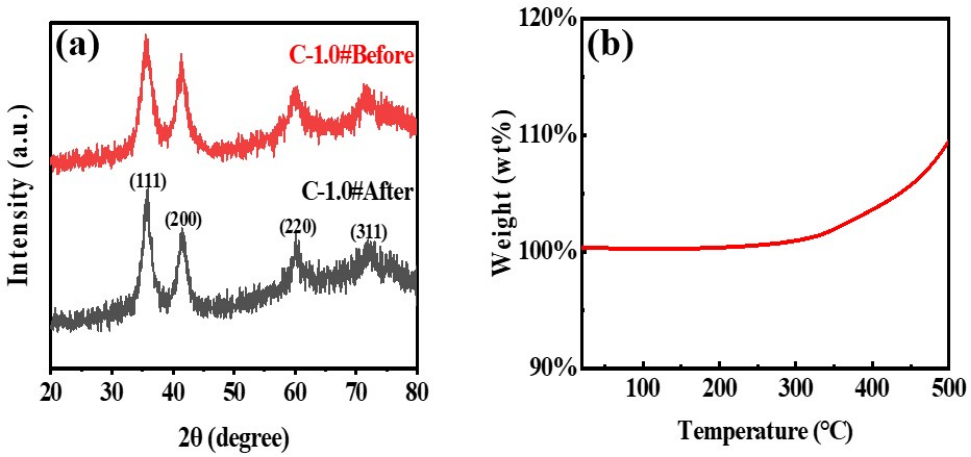

Fig. S2. (a) XRD patterns of $(Co_{0.2}Mo_{0.2}V_{0.2}Nb_{0.2}Ta_{0.2})C$ HECs before and after high temperature; **(b)** TGA curves of $(Co_{0.2}Mo_{0.2}V_{0.2}Nb_{0.2}Ta_{0.2})C$ HECs.

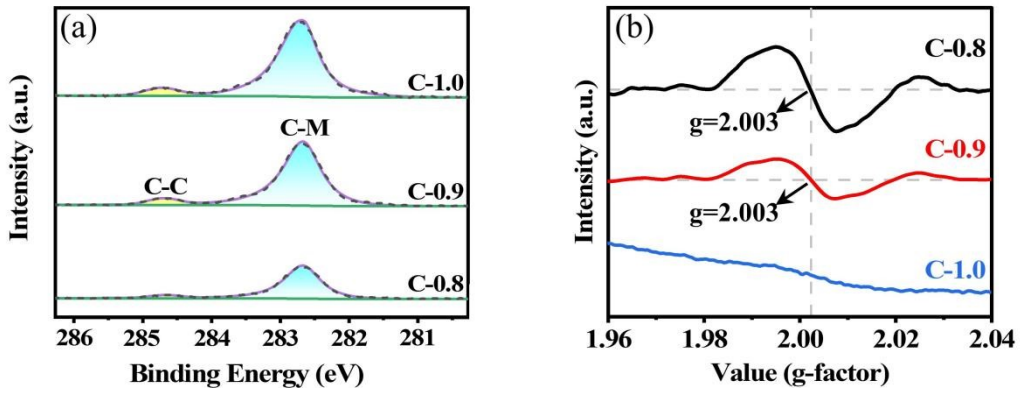

Fig. S3. (a) XPS data of C 1s of $(Co_{0.2}Mo_{0.2}V_{0.2}Nb_{0.2}Ta_{0.2})C_x$ with different graphite contents; **(b)** EPR curves of $(Co_{0.2}Mo_{0.2}V_{0.2}Nb_{0.2}Ta_{0.2})C_x$ with different graphite contents.

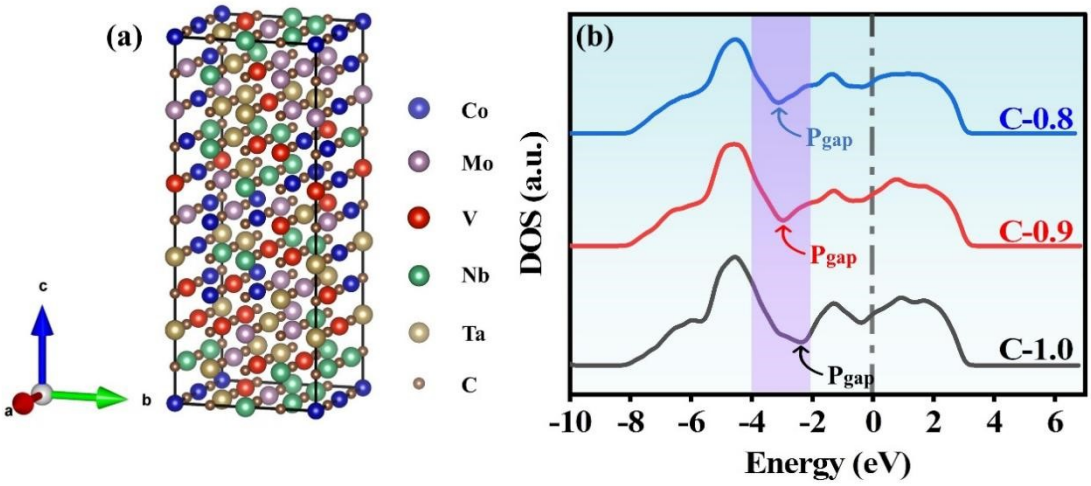

Fig. S4. (a) $(Co_{0.2}Mo_{0.2}V_{0.2}Nb_{0.2}Ta_{0.2})C$ supercell for density functional theory (DFT) calculations; **(b)** The density of states (DOS) of the $(Co_{0.2}Mo_{0.2}V_{0.2}Nb_{0.2}Ta_{0.2})C_x$.

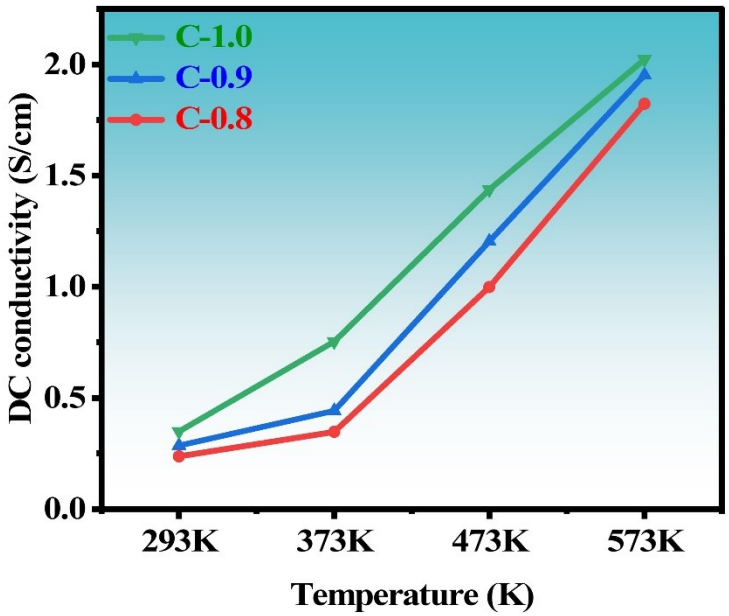

Fig. S5. Conductivity of $(Co_{0.2}Mo_{0.2}V_{0.2}Nb_{0.2}Ta_{0.2})C_x$ HECs in the temperature range of 293– 573 K.

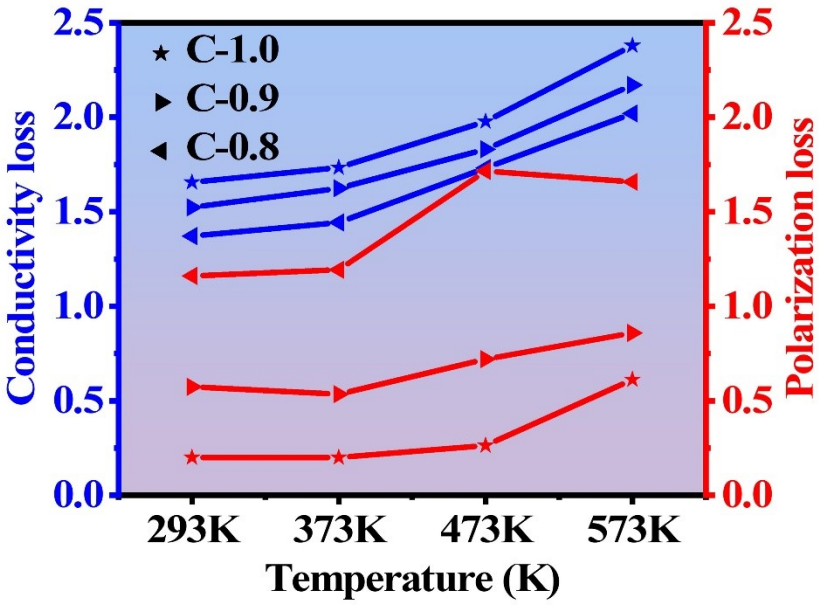

Fig. S6. Conductivity loss and polarization loss of $(Co_{0.2}Mo_{0.2}V_{0.2}Nb_{0.2}Ta_{0.2})C_x$ high-entropy ceramics at 293 K-573 K.

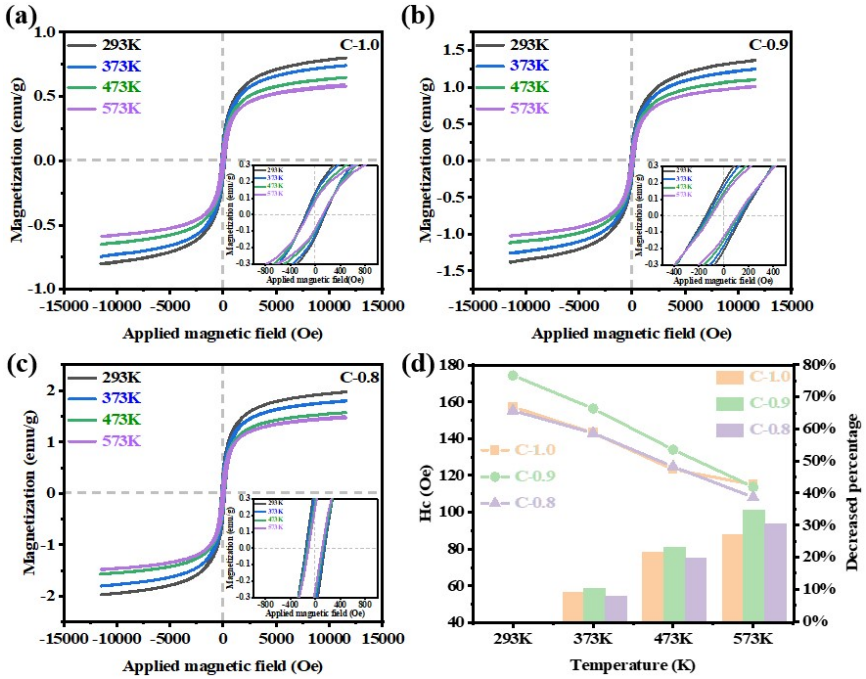

Fig. S7 (a-c) Hysteresis lines of samples at different temperatures. (d) Coercivity and its reduction at different temperatures

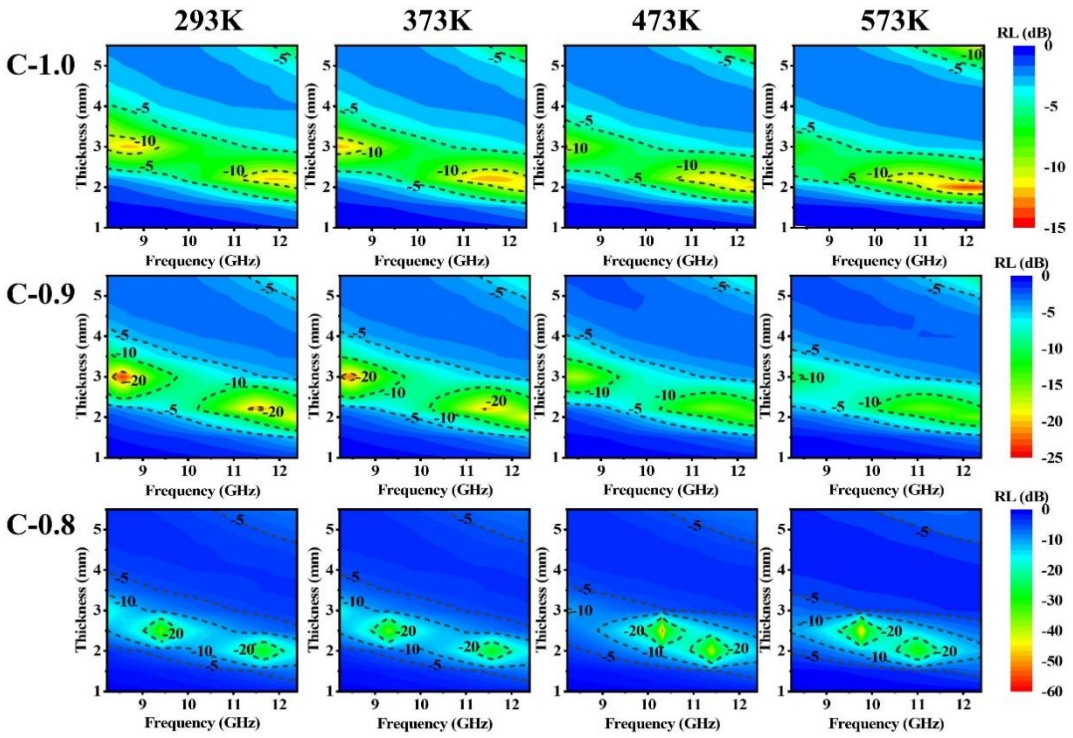

Fig. S8. *RL* values of $(Co_{0.2}Mo_{0.2}V_{0.2}Nb_{0.2}Ta_{0.2})C_x$ HECs at different temperatures with different thicknesses.

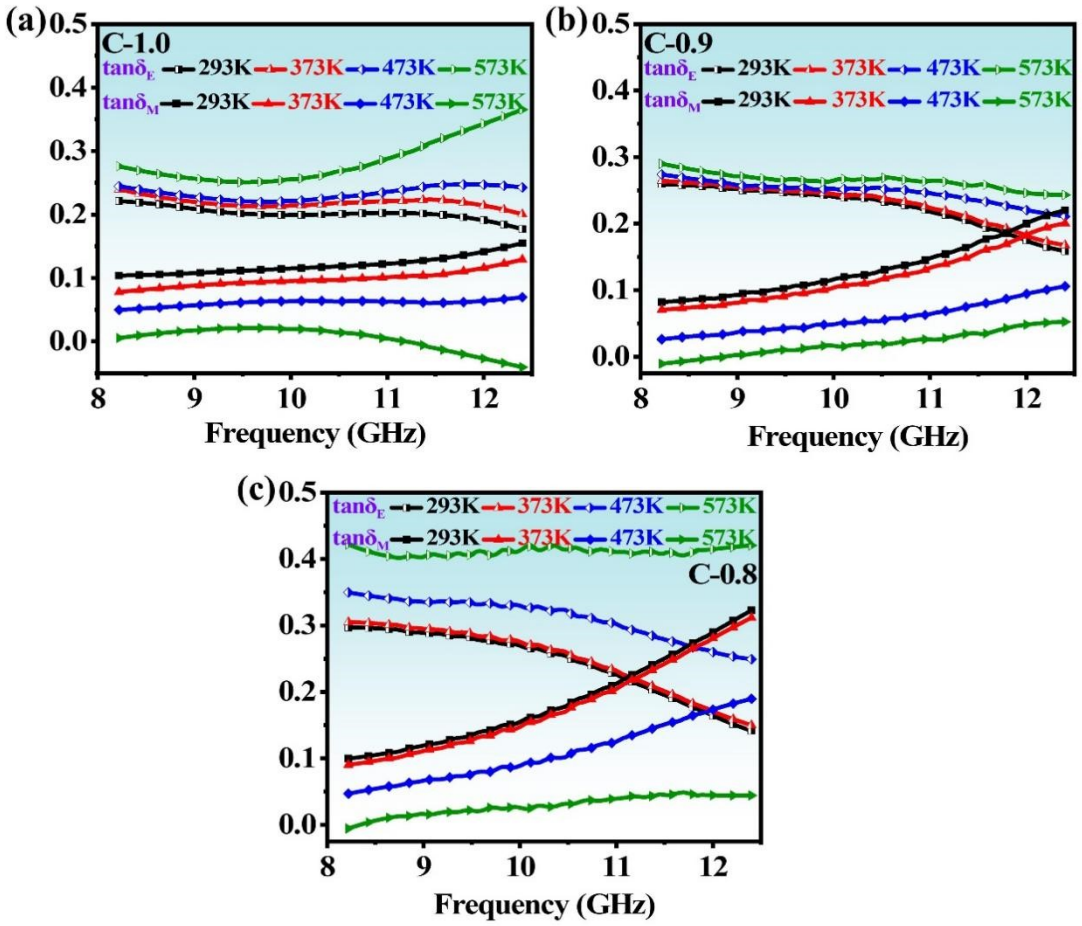

Fig. S9. Magnetic loss angle tangent ($tan\delta_M$) and dielectric loss angle tangent ($tan\delta_E$) of $(Co_{0.2}Mo_{0.2}V_{0.2}Nb_{0.2}Ta_{0.2})C_x$ HECs at different temperatures.

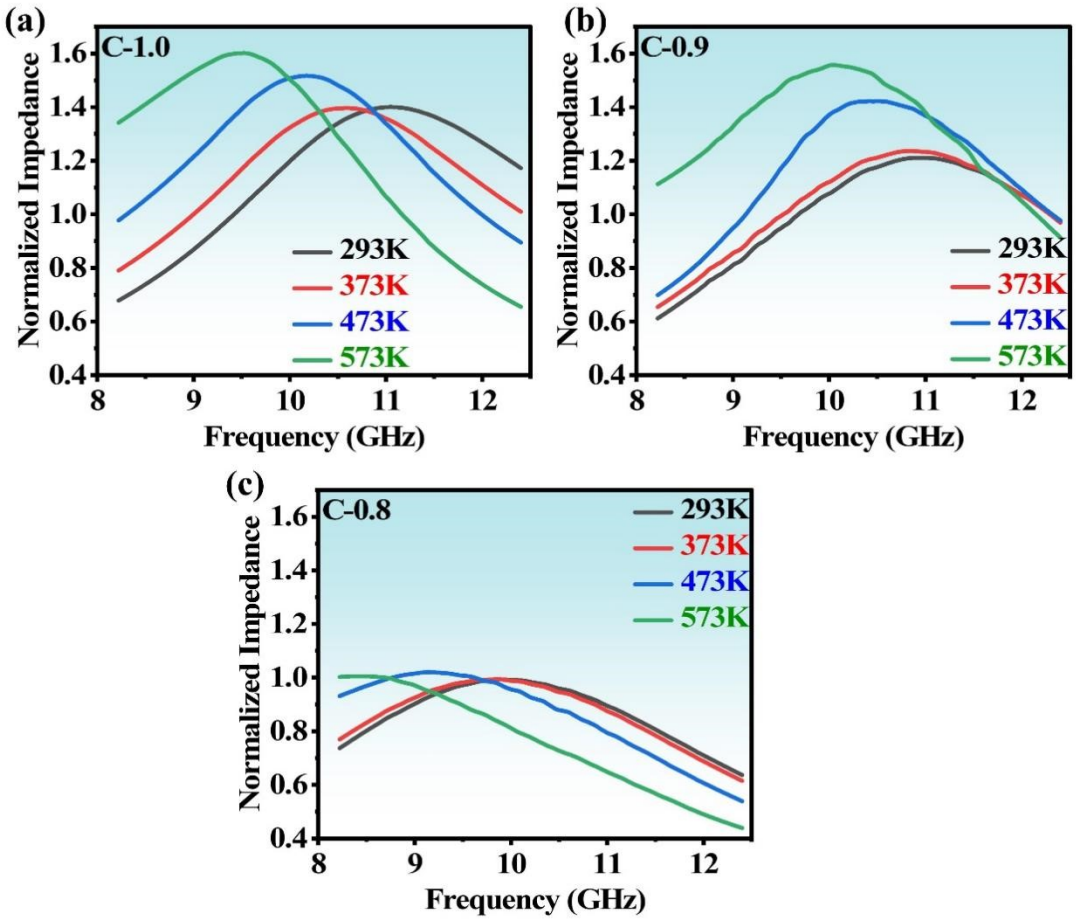

Fig. S10. Impedance matching curves of $(Co_{0.2}Mo_{0.2}V_{0.2}Nb_{0.2}Ta_{0.2})C_x$ HECs at different temperatures.

2. Supplementary Table

Table S1. Content of various elements in $(Co_{0.2}Mo_{0.2}V_{0.2}Nb_{0.2}Ta_{0.2})C$ high entropy ceramics

Element	wt%	at%
Co	10.71	9.64
Mo	18.32	10.12
V	9.03	9.40
Nb	16.06	9.16
Ta	33.73	9.88
C	11.58	51.08
Zr	0.42	0.24
O	0.15	0.48

Table S2. Carbon and oxygen content of $(Co_{0.2}Mo_{0.2}V_{0.2}Nb_{0.2}Ta_{0.2})C_mO_n$ HECs with their carbon, oxygen and vacancy stoichiometry.

Lable	C-1.0	C-0.9	C-0.8
C content (wt%)	10.16	9.67	9.23
O content (wt%)	0.12	0.16	0.19
C stoichiometry coefficient (m)	-	0.93	0.85
O stoichiometry coefficient (n)	-	0.02	0.02
Vacancies concentration (Vc, %)	-	5	13

Table S3. Typical high-temperature microwave absorption materials and their related performance.

Materials	RL_{min} (dB)	Maximum EAB (GHz)	Temperature stability (GHz)	Thickness (mm)	Ref.
Si_3N_4– SiC/SiO_2	−52.5	4.18	0.15	3.4	[1]
Fe-SiC/SiO_2	−14.0	3.40	3.30	3.0	[2]
TiN/BN/SiO_2	−17.0	3.26	0.99	2.0	[3]
TiN/ Fe_2Ni_2N/SiO_2	−22.0	3.89	0.36	2.8	[4]
Ni-SiC	−45.5	3.99	0.95	2.1	[5]
RGO/Si_3N_4	−16.5	4.20	0	4.3	[6]
Si_3N_4/SiC Aerogels	−45.0	4.20	0	4.0	[7]
FeCo@ZnO	−20.8	3.30	0.90	1.9	[8]
Ti_3SiC_2/Al_2O_3-13%TiO_2	−51.8	2.12	1.25	2.2	[9]
SiBCNHf	−15.0	3.67	0.27	2.6	[10]
C-0.8	−57.8	3.34	0.42	2.2	This work

3. Supplementary Note

1. Details of mixing of HECs with SiO_2 powder

Firstly, weigh the HECs powders and SiO_2 powders according to the mass percentage. Next, place the weighed powder into a beaker filled with alcohol. Then, perform ultrasonic treatment on the beaker for 30 minutes. Afterwards, dry and grind.

2. First-principles density functional theory (DFT) calculation methods

The density of states of $(Co_{0.2}Mo_{0.2}V_{0.2}Nb_{0.2}Ta_{0.2})C_x$ are investigated based on density functional theory (DFT) using the Vienna-Ab Initio Calculation Simulation Package (VASP). The solid solution structure of $(Co_{0.2}Mo_{0.2}V_{0.2}Nb_{0.2}Ta_{0.2})C_x$ is modeled using the Special Quasi-random Structure (SQS). In this study, a 2 × 2 × 5 SQS supercell with 160 atoms is generated using the "MCSQS" code of the Alloy Theoretic Automated Toolkit (ATAT). For the SQS model described above, a 4 × 4 × 4 Monkhorst k-point grid is adopted. The smearing (spreading) parameter and the plane wave energy cutoff is set to 0.2 eV and 400 eV, respectively. The exchange-correlation function is approximated using a Projector-Augmented Wave (PAW) potential and a modified Perdew-Burke-Ernzerhof (PBE) gradient. First, the structure is optimized without considering spin polarization, followed by static self-consistent and non-self-consistent calculations for the optimized structure based on spin polarization.

Supplementary References

[1] M. Li, X. Yin, G. Zheng, M. Chen, M. Tao, L. Cheng, L. Zhang, High-temperature dielectric and microwave absorption properties of Si_3N_4–SiC/SiO_2 composite ceramics, Journal of Materials Science, 50 (2014) 1478-1487.

[2] X. Yuan, L. Cheng, Y. Zhang, S. Guo, L. Zhang, Fe-doped SiC/SiO_2 composites with ordered inter-filled structure for effective high-temperature microwave attenuation, Materials & Design, 92 (2016) 563-570.

[3] Y. Shi, D. Li, H. Si, Z. Jiang, M. Li, C. Gong, TiN/BN composite with excellent thermal stability for efficiency microwave absorption in wide temperature spectrum, Journal of Materials Science & Technology, 130 (2022) 249-255.

[4] Y. Shi, D. Li, H. Si, Y. Duan, C. Gong, J. Zhang, TiN/Fe_2Ni_2N/SiO_2 composites for magnetic-dielectric balance to facilitate temperature-stable broadband microwave absorption, Journal of Alloys and Compounds, 918 (2022) 165603.

[5] J. Yuan, H. Yang, Z. Hou, W. Song, H. Xu, Y. Kang, H. Jin, X. Fang, M. Cao, Ni-decorated SiC powders: Enhanced high-temperature dielectric properties and microwave absorption performance, Powder Technology, 237 (2013) 309-313.

[6] Z. Hou, X. Yin, H. Xu, H. Wei, M. Li, L. Cheng, L. Zhang, Reduced Graphene Oxide/Silicon Nitride Composite for Cooperative Electromagnetic Absorption in Wide Temperature Spectrum with Excellent Thermal Stability, ACS Appl Mater Interfaces, 11 (2019) 5364-5372.

[7] Z. Cai, L. Su, H. Wang, M. Niu, L. Tao, Lu, L. Xu, M. Li, H. Gao, Alternating Multilayered Si_3N_4/SiC Aerogels for Broadband and High-Temperature

Electromagnetic Wave Absorption up to 1000 degrees C, ACS Appl Mater Interfaces, 13 (2021) 16704-16712.

[8] K. Peng, C. Liu, Y. Wu, G. Fang, G. Xu, Y. Zhang, C. Wu and M. Yan, *Journal of Materials Science & Technology*, 2022, **125**, 212-221.

[9] W.C. Wang, L.Y. Wang, G. Liu, C.Q. Ge, L. Wang, B. Wang, J. Huang, *Journal of the European Ceramic Society*, 2024, **44**, 254-260.

[10] Y. Song, Z.Y. Liu, X.C. Zhang, R.Q. Zhu, Y.W. Zhang, P.G. Liu, L.H. He, J. Kong, *Journal of Materials Science & Technology*, 2022, **126**, 215-227.